

Negative regulation of caspase 3-cleaved PAK2 activity by protein phosphatase 1

WANG JinJun^{1,2} & WANG ZhiXin^{1†}

¹ National Laboratory of Biomacromolecules, Institute of Biophysics, Chinese Academy of Sciences, Beijing 100101, China;

² Graduate University of Chinese Academy of Sciences, Beijing 100101, China

The p21-activated kinase 2 (PAK2) is activated by binding of small G proteins, Cdc42 and Rac, or through proteolytic cleavage by caspases or caspase-like proteases. Activation by both small G protein and caspase requires autophosphorylation at Thr-402 of PAK2. Although activation of PAK2 has been investigated for nearly a decade, the mechanism of PAK2 downregulation is unclear. In this study, we have applied the kinetic theory of substrate reaction during modification of enzyme activity to study the regulation mechanism of PAK2 activity by the catalytic subunit of protein phosphatase 1 (PP1 α). On the basis of the kinetic equation of the substrate reaction during the reversible phosphorylation of PAK2, all microscopic kinetic constants for the free enzyme and enzyme-substrate(s) complexes have been determined. The results indicate that (1) PP1 α can act directly on phosphorylated Thr-402 in the activation loop of PAK2 and down-regulate its kinase activity; (2) binding of the exogenous protein/peptide substrates at the active site of PAK2 decreases both the rates of PAK2 autoactivation and inactivation. The present method provides a novel approach for studying reversible phosphorylation reactions. The advantage of this method is not only its usefulness in study of substrate effects on enzyme modification but also its convenience in study of modification reaction directly involved in regulation of enzyme activity. This initial study should provide a foundation for future structural and mechanistic work of protein kinases and phosphatases.

p21-activated protein kinase, substrate reaction kinetics, phosphorylation, dephosphorylation

The p21-activated kinases (PAKs) 1–3 are serine/threonine protein kinases defined by their interaction with the small GTPases, Cdc42 and Rac^[1]. PAKs play an important role in diverse cellular processes, including cytoskeletal dynamics, growth/apoptotic signal transduction through mitogen-activated protein kinases, and regulation of transcription factors^[2–4]. All PAKs consist of a C-terminal kinase domain and an N-terminal regulatory domain containing a GTPase binding domain and an inhibitory domain. These p21 G proteins in the GTP-bound state bind to a conserved region within the N-terminal regulatory domain of PAKs and release inhibition of the catalytic site by an overlapping autoinhibitory domain. PAKs are activated by the binding of active Cdc42 and Rac to the GTPase binding domain, resulting

in a conformational change and a subsequent autophosphorylation on several serine and/or threonine residues.

The ubiquitous PAK2 is unique among the PAK family because it is also activated through proteolytic cleavage by caspases or caspase-like proteases^[5,6]. Proteolytic cleavage removes most of the N-terminal regulatory domain including the autoinhibitory domain and generates constitutively active PAK2-p34, a 34-kDa C-terminal fragment that contains the entire catalytic domain. Activation by both Cdc42 and caspases requires autophosphorylation at Thr-402 of PAK2. Caspase activation has not been demonstrated for any other PAK

Received May 22, 2007; accepted November 11, 2007

doi: 10.1007/s11427-008-0006-z

†Corresponding author (email: zxwang@sun5.ibp.ac.cn)

Supported by the National Natural Science Foundation of China (Grant No. 30230100)

isoform and among the PAK family appears to be a unique characteristic for PAK2. In response to stress stimulants such as tumor necrosis factor α or growth factor withdrawal, PAK2 is activated as a full length enzyme and as a proteolytic PAK2-p34 fragment. Activation of full-length PAK2 stimulates cell survival and cell growth, whereas proteolytic activation of PAK2-p34 is involved in programmed cell death^[7,8].

The importance of phosphorylation in PAK activation suggests that dephosphorylation reactions will be equally important in shutting off PAK activity. Protein Ser/Thr phosphatases fall into two structurally distinct sub-gene families, PPP and PPM^[9]. The PPP subfamily includes protein phosphatase 1 (PP1), 2A (PP2A), and 2B (PP2B, also called calcineurin). The PPM family consists of the Mg^{2+}/Mn^{2+} -dependent PP2C-like enzymes. PP1 is a member of the PPP gene family, whose members share 40% sequence identity in the catalytic subunit. Many studies have implicated an important regulatory role for PP1 in a wide variety of cellular function including metabolism, transcription and translation, ion transport, development, cell growth, and differentiation^[10]. Considerable effort has been made to understand the mechanisms of PAK down-regulation at the molecular level. Westphal et al.^[11] showed that in rat brain, PP2A could associate with PAK1 and PAK3 to form a binary complex. Using bacterial-expressed partially phosphorylated GST-PAK3, Zhan et al.^[12] demonstrated that PP1 α and PP2A acted directly on Thr-421 in PAK3 (equivalent to Thr-402 in PAK2). Koh et al.^[13] reported two PP2C-like serine/threonine phosphatases (POPX1 and POPX2) that efficiently inactivated PAK1 *in vitro*. The dephosphorylating activity of POPX correlated with an ability to block the *in vivo* effects of active PAK. However, the phosphatases against PAK2 have not been studied *in vitro* until now.

In this study, we have applied the kinetic theory of substrate reaction during modification of enzyme activity^[14-16] to study the regulation mechanism of PAK2 activity by the catalytic subunit of protein phosphatase 1 (PP1 α). On the basis of the kinetic equation of the substrate reaction during the reversible phosphorylation of PAK2, all microscopic kinetic constants for the free enzyme and enzyme-substrate(s) complexes have been determined. The results indicate that (i) PP1 α can act directly on phospho-Thr402 in the activation loop of PAK2 and down-regulate its kinase activity; (ii) binding

of the exogenous protein/peptide substrates at the active site of PAK2 decreases both the rates of PAK2 autoactivation and inactivation.

1 Experimental procedures

1.1 Materials

Adenosine 5'-triphosphate (ATP), *p*-nitrophenyl phosphate, bovine brain acetone powder, phospho(enol)pyruvate (PEP), nicotinamide adenine dinucleotide (reduced) (NADH), lactate dehydrogenase (LDH), pyruvate kinase (PK), purine nucleoside phosphorylase, and the ingredients to generate the phosphorylase substrate, 2-amino-6-mercapto-7-methylpurine ribonucleoside (MESG), were purchased from Sigma. MESG was synthesized according to the procedures described by Killilea et al.^[17]. Fetal bovine serum, Grace's insect cell culture medium and yeastolate solution were purchased from Gibco-BRL, 3-(N-morpholino)propane sulfonic acid (MOPS) and Tris were purchased from Boehringer Mannheim. Other reagents were local products of analytical grade used without further purification. Double-deionized water was used throughout.

1.2 Expression and purification of proteins

GST-fusion human PAK2 was expressed in Sf9 cells and purified as described previously^[18]. A constitutively active Cdc42, GST-Cdc42L61 was expressed in *E. coli* and purified according to standard procedures using the affinity matrix Glutathione Sepharose 4B (Amersham Pharmacia Biotech). The recombinant catalytic subunit of protein phosphatase 1 (PP1 α) was expressed in *E. coli* as described by Zhang et al.^[19]. The N-terminal His₆-tagged caspase 3 was expressed in *E. coli* BL21 (DE3) and purified using standard procedures of nickel chelate affinity chromatography^[20]. The protein purity was over 90% as judged by SDS-PAGE. Protein concentrations were determined according to the method of Bradford with bovine serum albumin (BSA) as a standard. The purified proteins were made to 20% glycerol and stored at -80°C . Myelin basic protein (MBP) was isolated from brain acetone powder based on a published protocol^[21]. Protein concentration determination was based on an extinction coefficient calculated from the amino acid composition of bovine MBP, $\epsilon_{280} = 10800 \text{ (mol/L)}^{-1} \cdot \text{cm}^{-1}$ ^[22].

1.3 Enzyme assays for PP1 α

With *p*-nitrophenyl phosphate (pNPP) as a substrate, the reaction was initiated by the addition of the enzyme in a reaction mixture, and the initial rates for hydrolysis of pNPP by PP1 α were measured at 30°C in pH 7.4 buffer containing 100 mmol/L MOPS, 1 mmol/L DTT, 100 mmol/L KCl, and 20 mmol/L MgCl₂. The nonenzymatic hydrolysis of the substrate was corrected by measuring the control without the addition of enzyme. The amount of product *p*-nitrophenol was determined from the absorbance at 405 nm using a molar extinction coefficient of 18000 (mol/L)⁻¹·cm⁻¹[23]. Kinetic parameters for the dephosphorylation of the phosphorylated myelin basic protein (pMBP) was determined using a continuous spectrophotometric assay^[24,25]. All experiments were carried out at 30°C in pH 7.4 buffer containing 100 mmol/L MOPS, 1 mmol/L DTT, 100 mmol/L KCl, 20 mmol/L MgCl₂, 200 μmol/L MESG and 1 unit/mL purine nucleoside phosphorylase. Quantitation of inorganic phosphate produced in the phosphatase reaction was determined using the extinction coefficient of 11050 (mol/L)⁻¹·cm⁻¹ at 360 nm and pH 7.4^[26].

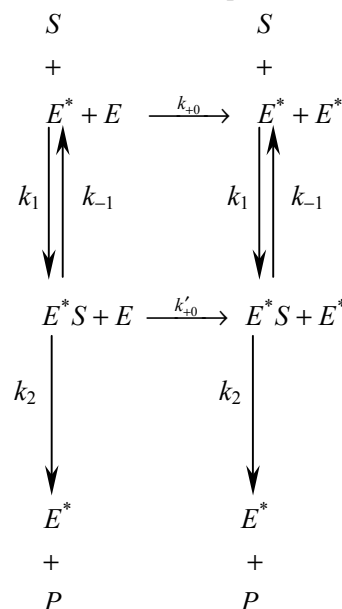
1.4 Enzyme assays for PAK2

Enzyme activity of PAK2 was determined with the MBP or peptide (RLCtide, KKRPRQATSNVFA) as a substrate using a coupled spectrophotometric assay, except where indicated^[27]. The standard assay for PAK2 was carried out at 30°C in 1.8 mL reaction mixture containing 100 mmol/L MOPS buffer, pH 7.4, 100 mmol/L KCl, 20 mmol/L MgCl₂, 1.5 mmol/L ATP, 1 mmol/L DTT, 200 μmol/L NADH, 1 mmol/L phospho(enol)pyruvate, 20 units/mL lactate dehydrogenase, 15 units/mL pyruvate kinase, and different concentrations of substrates. Reactions were initiated by the addition of PAK2 to the reaction mixture. Progress of the reaction was monitored continuously by following the formation of NAD⁺ at 340 nm, on a PerkinElmer Lambda 45 spectrophotometer. The concentrations of ADP formed in PAK2-catalyzed reaction were determined using an extinction coefficient for NADH of 6220 (mol/L)⁻¹·cm⁻¹ at 340 nm. The concentrations of substrates and PAK2 are given in the text or in the legends to the figures. The peptide was synthesized using standard protocol, purified by reverse-phase preparative HPLC chromatography, and characterized by MALDI-TOF mass spectrometry by ADI Inc. The concentration of peptide was determined

by turnover with the GST-PAK2 under conditions of limiting peptide.

2 Kinetic analysis

In the presence of exogenous substrate, the general mechanism of the intermolecular autophosphorylation at low enzyme concentrations can be represented by Scheme 1

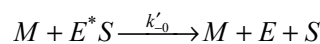
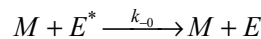


Scheme 1

where *E* and *E*^{*} represent unphosphorylated and phosphorylated enzyme, and *S* and *P* represent exogenous substrate and its corresponding product, respectively. If the phosphorylated enzyme can be dephosphorylated mediated by a protein phosphatase, two more reactions should be included into Scheme 1,



where *M* represents the phosphatase. At low [*M*]₀, [*T*]₀, where [*M*]₀, [*T*]₀ << *K*_s and *K*'_s, the reactions can then be written as



where *k*₋₀ = *k*_c/*K*_s and *k*'₋₀ = *k*'_c/*K*'_s are the apparent second-order rate constants for dephosphorylation reactions. If we assume that (1) the enzymatic reaction is irreversible and not inhibited by the product formed, (2) the substrate concentration remains constant throughout the activity measurement, (3) the product concentration is

much less than the corresponding Michaelis constant for M ($[P] \ll K_p$), and (4) the steady-state of the substrate reaction is rapidly established, application of the steady-state treatment to E^*S gives rise to

$$K_m = \frac{[E^*][S]}{[E^*S]}, \quad (1)$$

where $K_m = (k_{-1} + k_2)/k_1$ is the Michaelis constant for the exogenous substrate. Let

$$[E_T^*] = [E^*] + [E^*S]. \quad (2)$$

The total concentration of enzyme is

$$[T]_0 = [E^*] + [E^*S] + [E] = [E^*]_0 + [E]_0, \quad (3)$$

where $[E]_0$ and $[E^*]_0$ are the initial concentrations of the unphosphorylated and phosphorylated enzyme, respectively. $[T]_0$ is the total enzyme concentration in the assay system. From eqs. (1)–(3), we have

$$[E^*] = \frac{K_m[E_T^*]}{K_m + [S]}, \quad (4)$$

$$[E^*S] = \frac{[E_T^*][S]}{K_m + [S]}. \quad (5)$$

The rate of the phosphorylated enzyme formation is given by

$$\begin{aligned} \frac{d[E_T^*]}{dt} &= k_{+0}[E^*][E] + k'_{+0}[E^*S][E] \\ &\quad - k_{-0}[M]_0[E^*] - k'_{-0}[M]_0[E^*S] \\ &= \frac{k_{+0}K_m + k'_{+0}[S]}{K_m + [S]}[E_T^*][E] \\ &\quad - \frac{k_{-0}K_m + k'_{-0}[S]}{K_m + [S]}[E_T^*][M]_0 \\ &= A[E_T^*][E] - B[M]_0[E_T^*] \\ &= A[E_T^*]([T]_0 - [E_T^*]) - B[M]_0[E_T^*] \\ &= (A[T]_0 - B[M]_0)[E_T^*] - A[E_T^*]^2 \\ &= k_{\text{obs}}^*[E_T^*] - A[E_T^*]^2, \end{aligned} \quad (6)$$

where

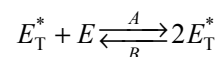
$$A = \frac{k_{+0}K_m + k'_{+0}[S]}{K_m + [S]}, \quad (7)$$

$$B = \frac{k_{-0}K_m + k'_{-0}[S]}{K_m + [S]}, \quad (8)$$

$$k_{\text{obs}}^* = A[T]_0 - B[M]_0. \quad (9)$$

Note that when the consumption of substrate is negligible during the course of reaction, A and B can be regarded as apparent rate constants of the following reac-

tion:



With the boundary conditions, $t=0$, $[E_T^*] = [E^*]_0$, eq. (6) can be integrated to give

$$[E_T^*] = \frac{k_{\text{obs}}^*[E^*]_0}{A[E^*]_0 + (k_{\text{obs}}^* - A[E^*]_0)e^{-k_{\text{obs}}^*t}}. \quad (10)$$

The rate of product formation while the enzyme is being modified is

$$\begin{aligned} \frac{d[P]}{dt} &= k_2[E^*S] = \frac{k_2[S][E_T^*]}{K_m + [S]} \\ &= \frac{k_2[S]k_{\text{obs}}^*[E^*]_0}{(K_m + [S])\{A[E^*]_0 + (k_{\text{obs}}^* - A[E^*]_0)e^{-k_{\text{obs}}^*t}\}} \end{aligned} \quad (11)$$

The concentration of product formed at time t is given by

$$[P] = \frac{v_s^*}{k_{\text{obs}}^*} \ln \left\{ 1 - \frac{\alpha A[T]_0}{k_{\text{obs}}^*} (1 - e^{k_{\text{obs}}^*t}) \right\}, \quad (12)$$

where

$$\alpha = [E^*]_0/[T]_0, \quad (13)$$

$$v_s^* = \frac{k_2[T]_0[S]}{K_m + [S]} \frac{A[T]_0 - B[M]_0}{A[T]_0}. \quad (14)$$

It can be verified that when $t \rightarrow \infty$, eq. (12) approach an oblique asymptote

$$[P] = v_s^*t - \frac{v_s^*}{k_{\text{obs}}^*} \ln \frac{A[T]_0\alpha}{k_{\text{obs}}^*}. \quad (15)$$

From this equation, the steady-state rate, v_s^* , can be obtained. In the absence of PP1 α ($[M]_0 = 0$), eq. (12) becomes

$$[P] = \frac{v_s}{k_{\text{obs}}} \ln \left\{ 1 - \alpha(1 - e^{k_{\text{obs}}t}) \right\}, \quad (16)$$

where

$$v_s = \frac{k_2[T]_0[S]}{K_m + [S]}, \quad (17)$$

$$k_{\text{obs}} = A[T]_0 = \frac{k_{+0}K_m + k'_{+0}[S]}{K_m + [S]}[T]_0. \quad (18)$$

3 Results

3.1 Steady-state kinetics of protein phosphatase 1 catalyzed reaction

To understand the molecular basis of the regulation of

caspase 3-cleaved PAK2 activity by PP1 α , steady-state parameters for the PP1 α -catalyzed hydrolysis of pNPP and phosphorylated MBP (pMBP) were first determined at pH 7.4 and 30°C. Figure 1(a) shows initial rates of PP1 α -catalyzed reaction as a function of the concentrations of pNPP or pMBP. The initial velocity gives rise to the hyperbolic dependence on the pNPP concentration. The experimental data fit the Michaelis-Menten equation with a K_m of 15.4 \pm 2.0 mmol/L, and k_{cat} of 11.7 \pm 0.7 s $^{-1}$. To determine the kinetic parameters for the pMBP hydrolyzing activity of PP1 α , MBP (1 mmol/L) was phosphorylated by GST-PAK2 (20 nmol/L) for 60 min at 30°C under kinetically valid conditions (100 mmol/L MOPS, pH 7.4, 1 mmol/L DTT, 100 mmol/L KCl, 20 mmol/L MgCl $_2$, 10 mmol/L ATP). The phosphorylation of MBP (169 amino acids) by PAK2 has been mapped to single site Ser-55^[28]. The assay for PP1 α activity was measured by following the P $_i$ release using an enzyme coupled spectrophotometric method^[24,25]. The experimental data fit well with the Michaelis-Menten equation yielding $K_m=7.1\pm 0.8 \mu\text{mol/L}$, $k_{cat}=14.0\pm 0.8 \text{ s}^{-1}$, respectively. In order to study the effect of MBP on PP1 α -catalyzed reaction, the initial rates of the PP1 α -catalyzed pNPP and pMBP hydrolysis in the presence of various concentrations of MBP were measured. Figure 1(b) shows the dependence of the initial rates of the PP1 α -catalyzed reactions on the MBP concentration. As shown in this figure, progressive addition of MBP does not affect the rates of PP1 α -catalyzed reactions. This result suggests that either binding of MBP to PP1 α is

negligible or the binary complex of PP1 α -MBP has similar enzyme activity as the free enzyme.

3.2 Kinetics of substrate reaction during autocatalytic activation of PAK2

Recombinant GST-PAK2 from human was expressed in insect cell as an inactive enzyme, and can be activated by cleavage with caspase 3 or by binding of Rho family small G proteins, Cdc42 or Rac. These two activation mechanisms may involved in different signal transduction pathways. Upon activation, PAK2 from rabbit is autophosphorylated at eight sites^[29]. Seven autophosphorylation sites on serine have been identified in the N-terminal regulatory domain by microsequence analysis. In the C-terminal catalytic domain, a single phosphothreonine is observed, Thr-402. To determine whether autophosphorylated PAK2 is a substrate for PP1 α *in vitro*, the GST-PAK2 (3 $\mu\text{mol/L}$) was incubated with 5 mmol/L ATP, 20 mmol/L MgCl $_2$ and 15 $\mu\text{mol/L}$ Cdc42L61 at 30°C, and autophosphorylation of GST-PAK2 was analyzed by SDS-PAGE^[16]. The fully phosphorylated and activated enzyme ran as a single 97 kDa band on a 7.5% polyacrylamide gel (Lane 3 in Figure 2), shifted by 13 kDa from the inactive form that ran 84 kDa (Lane 2 in Figure 2). After PAK2 autophosphorylation, ATP was removed by gel filtration and the activated PAK2 was incubated with 1 $\mu\text{mol/L}$ PP1 α for 30 min. PP1 α potentially dephosphorylated PAK2, as evidenced by a downward mobility shift of the PAK2 band by SDS-PAGE (Lane 4 in Figure 2).

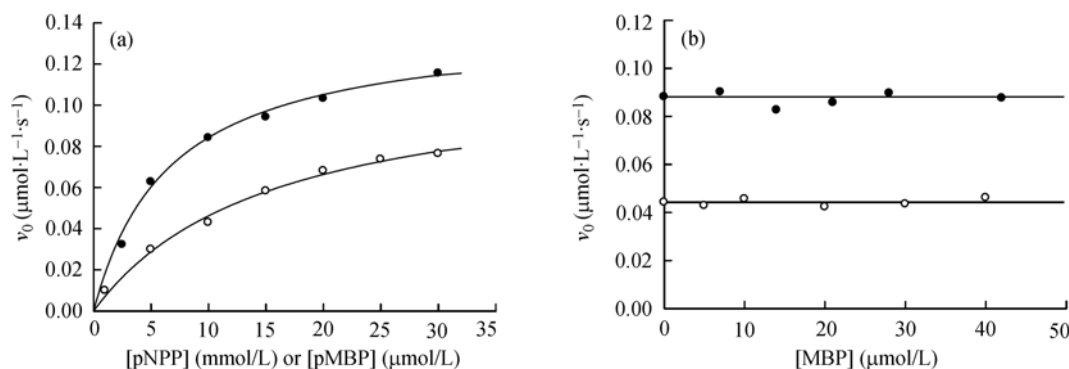


Figure 1 Dependence of the initial velocity on pNPP, pMBP and MBP for the PP1 α -catalyzed reaction. (a) Plot of v_0 versus pNPP (○) or pMBP (●) concentration. All experiments were performed at 30°C, pH 7.4 in 100 mmol/L MOPS buffer (see section 1). The reaction was initiated by addition of 10 nmol/L PP1 α . The solid lines are best fitting results according to the Michaelis-Menten equation. (b) Effect of MBP concentration on the initial velocity of the PP1 α -catalyzed reaction with 10 mmol/L pNPP (○) or 14 $\mu\text{mol/L}$ pMBP (●) as the substrate. All experiments were performed at 30°C, pH 7.4 in 100 mmol/L MOPS buffer (see section 1). 10 nmol/L PP1 α was added to the reaction mixture to start the reaction.

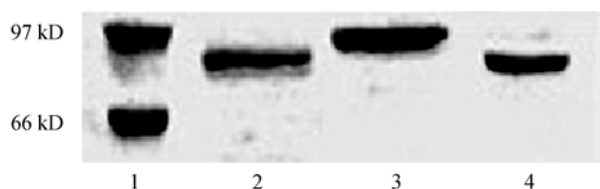


Figure 2 SDS-PAGE of unphosphorylated and phosphorylated GST-PAK2. Lane 1, molecular mass markers of 97.4 and 66.2 kDa, respectively; Lane 2, unphosphorylated GST-PAK2; Lane 3, phosphorylated GST-PAK2; Lane 4, dephosphorylated GST-PAK2.

In order to confirm that PP1 α acts on PAK2 phosphorylation at Thr-402, the kinetic theory of the substrate reaction during modification of enzyme activity was applied to a study of the inactivation of PAK2 by PP1 α . Walter et al.^[6] have shown that *in vitro*, caspase 3 cleaves recombinant PAK2 into two peptides: p27 (1–212) contains the majority of the regulatory domain and p34 (212–524) contains 34 amino acids of the regulatory domain plus the entire catalytic domain. Following cleavage, both peptides become autophosphorylated with MgATP alone. Thr-402 was the only detectable site of autophosphorylation in p34, and enzyme activation coincides with autophosphorylation of this site. To directly investigate the role of Thr-402 in PAK2 activation, in the studies described here, all kinetic experiments were carried out with caspase 3-cleaved p34 peptide. The full-length GST-PAK2 (p90) was incubated with caspase 3 (1 μ mol/L) for 30 min, and the reaction mixture was analyzed by SDS-PAGE. As shown by Coomassie Blue stain, p90 was cleaved into two peptides, p53 and p34 on SDS-PAGE (Lanes 1 and 2 in Figure 3). As indicated by Walter et al. that the peptide of 53000 dalton (p53) contained GST-p27. Figure 4(a) shows the time courses of PAK2-catalyzed reaction at different enzyme concentrations when an aliquot of the caspase 3-cleaved PAK2 was added to assay system. Preincubation of caspase 3-cleaved PAK2 with MgATP leads to a linear progress curve (see Figure 4(a), control), indicating that the substrate consumption can be neglected and the initial rate conditions are satisfied during activity measurement. Because the enzyme concentration in the assay system is far less than the inhibition constant of the N-terminal domain ($K_i = \sim 90$ nmol/L), proteolysis would be expected to actually release the catalytic domain^[30]. In the previous study, we have shown that PAK2 activation is related to an intermolecular autophosphorylation event^[16], and the time-dependent behavior of enzyme-catalyzed

reaction can be well described by eq. (16) when the substrate consumed is negligible. Therefore, the values of v_s , α and k_{obs} can be determined by fitting this equation to the experimental data. Figure 4(b) shows the effects of the PAK2 concentration on v_s and k_{obs} . As expected, both of them are proportional to the enzyme concentration.

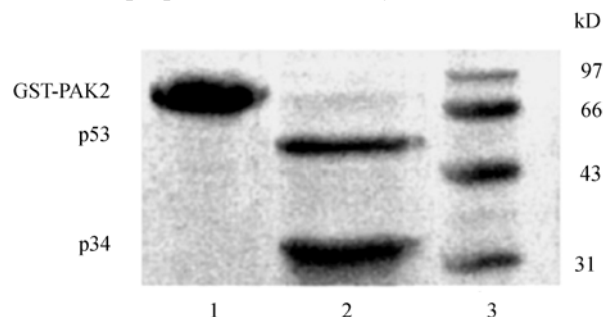


Figure 3 Identification of the cleavage products of GST-PAK2 by caspase 3. GST-PAK2 (p90) was incubated in the absence and presence of caspase 3. The protein and its cleavage products were identified by Coomassie stain and are indicated by molecular mass. Lane 1, GST-PAK2 alone; Lane 2, GST-PAK2 plus caspase 3; Lane 3, molecular mass markers of 97, 66, 43, and 31 kDa, respectively.

Figure 5(a) shows the time courses of product formation at a fixed PAK2 concentration and different PP1 α concentrations. Similarly, the progress curves start off the lag phases, and go up with increasing time due to the activation of PAK2. When reaction time is sufficiently large, the curves approach straight lines the slopes of which are equal to the steady-state rates of PAK2-catalyzed reaction. Under the conditions employed in the present study, the time-dependent behavior of enzyme-catalyzed reaction can be described by eq. (12). It can be seen from this equation that any particular progress curve contains four kinetic parameters, A , v_s^* , α and k_{obs}^* . In theory, the fitting of data from a single progress curve to eq. (12) by the non-linear least-squares method will yield values for these parameters. However, eq. (12) is quite complex and, due to the fact that experimental data always contain experimental uncertainties, may be difficult to treat by the conventional single-curve fitting procedure. With a set of unfortunate starting values, the fitting procedure will converge to the wrong values. Therefore, it is necessary to constrain one or more parameters to constant values. Since the value of A can be determined separately from the experiments in the absence of PP1 α , we can fix it to a constant value in curve fitting. The best-fit curves in Figure 5(a) were obtained by nonlinear regression analysis from which the kinetic

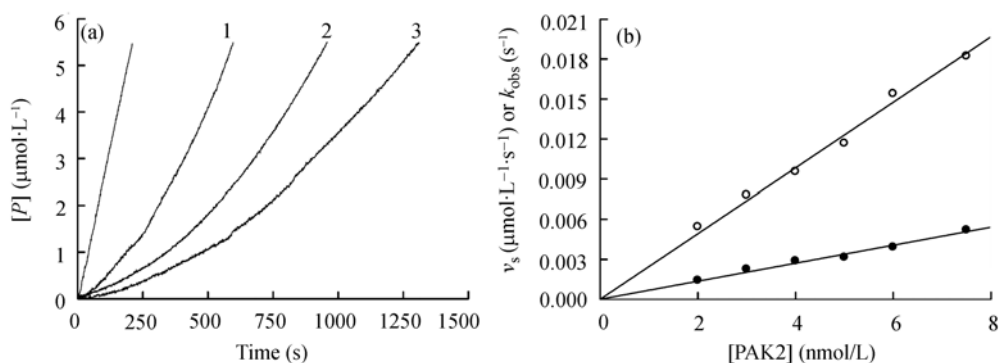


Figure 4 Time course of substrate reaction in the presence of different concentrations of PAK2-p34. (a) The full-length GST-PAK2 was incubated with caspase 3 (1 μmol/L) for 30 min, and an aliquot was taken out and added to the reaction mixture to start the reaction. The reaction mixture contained 100 mmol/L MOPS buffer, pH 7.4, 100 mmol/L KCl, 10 mmol/L MgCl₂, 200 μmol/L NADH, 1 mmol/L phospho(enol)pyruvate, 20 units/mL lactate dehydrogenase, 15 units/mL pyruvate kinase, 30 μmol/L MBP and 1.5 mmol/L ATP. All experiments were performed at 30°C. The enzyme concentrations were 7.5 nmol/L (curve 1), 5 nmol/L (curve 2) and 3 nmol/L (curve 3), respectively. In the control experiment, the full-length GST-PAK2 was preincubated with caspase 3 and MgATP, 7.5 nmol/L fully activated p34 peptide was used to initiate the reaction. The data were fitted to eq. (16) to determine the kinetic parameters, v_0 , A and α . (b) Plots of the v_s (○) and k_{obs} (●) versus enzyme concentration.

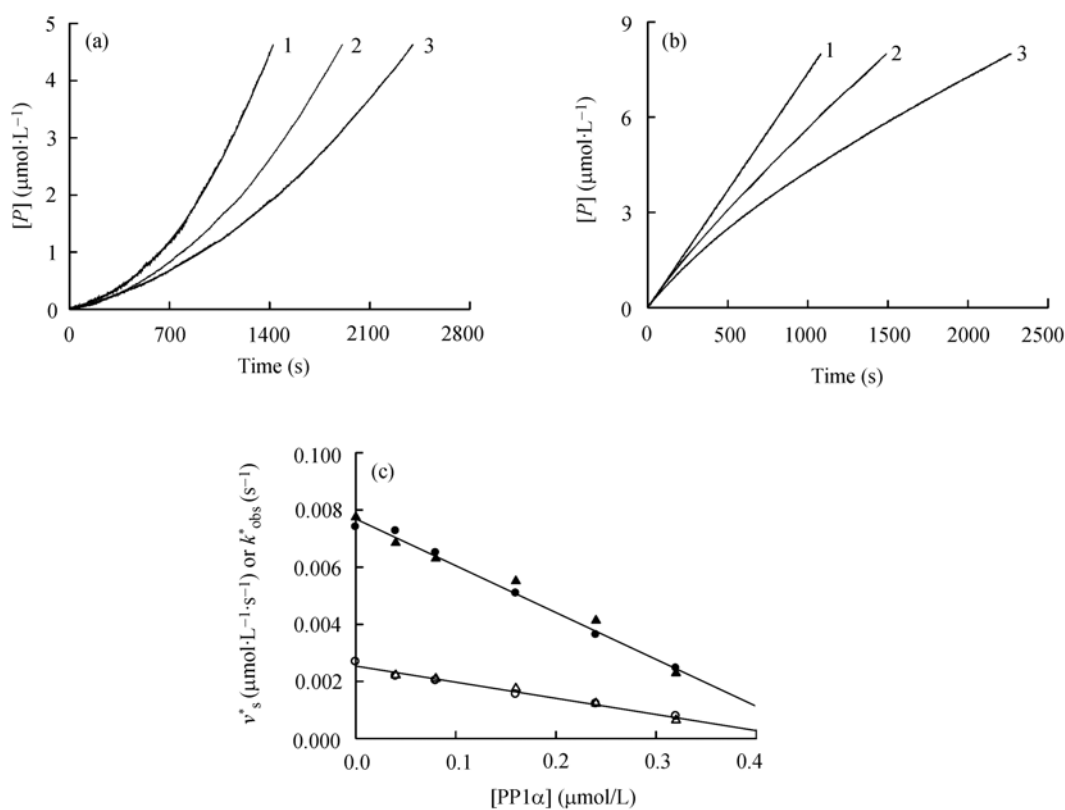


Figure 5 Time course of substrate reaction in the presence of different concentrations of PP1 α . All experiments were performed at 30°C. Reaction mixture contained 100 mmol/L MOPS buffer, pH 7.4, 100 mmol/L KCl, 20 mmol/L MgCl₂, 200 μmol/L NADH, 1 mmol/L DTT, 1 mmol/L phospho(enol)pyruvate, 20 units/mL lactate dehydrogenase, 15 units/mL pyruvate kinase, 20 μmol/L MBP, 3 nmol/L PAK2-p34, 1.5 mmol/L ATP and different concentration PP1 α . The kinetic parameters v_s^* , k_{obs}^* and α were determined by fitting eq. (12) to the experimental data, where A was fixed to a constant value obtained from the control experiment (curve 1). (a) The reaction was started by the addition of PAK2-p34. Concentrations of PP1 α were 0 nmol/L (curve 1), 160 nmol/L (curve 2), and 240 nmol/L (curve 3), respectively. (b) The reaction was started by the addition of phosphorylated PAK2-p34. Concentrations of PP1 α were 0 nmol/L (curve 1), 160 nmol/L (curve 2), and 320 nmol/L (curve 3), respectively. (c) Plots of v_s^* (●, ▲) and k_{obs}^* (○, △) versus PP1 α concentration. The circles and triangles were obtained from (a) and (b), respectively.

parameters, v_s^* , α and k_{obs}^* can be determined. Alternatively, the reactions can also be initiated by adding the fully phosphorylated active PAK2. Figure 5(b) shows the time courses of PAK2-catalyzed MBP phosphorylation reaction in the presence of different concentrations of PP1 α . The progress curves starts off linear (the initial-rate phase) but falls off with increasing time due to the action of PP1 α . When t approaches infinity, $[P]$ approaches an asymptote with a positive slope. The slopes of the straight lines decrease with increasing PP1 α concentrations, indicating that the dephosphorylation of PAK2 is a reversible process. Similarly, from the progress curves, v_s^* , α and k_{obs}^* can be determined by fitting the experimental data to eq. (12) with $\alpha = [E^*]_0/[T]_0 = 1$. Figure 5(c) shows the effects of the PP1 α concentration on the steady-state rate, v_s^* and the apparent inactivation rate constant, k_{obs}^* . With increase in the concentration of PP1 α , v_s^* decreases linearly. The steady-state rate decreased from 0.0077 to 0.0025 $\mu\text{mol/L}\cdot\text{s}^{-1}$ when the concentration of PP1 α was increased from 0 to 320 nmol/L. The value of k_{obs}^* is also linear function of PP1 α concentration. The linear relationship between k_{obs}^* and enzyme concentration suggests that in the present study, the conditions that $[M]_0$, $[T]_0 \ll K_s$ and K'_s are satisfied. It can be seen from Figure 5(c) that the values of v_s^* and k_{obs}^* obtained from the two different procedures are comparable with each other.

3.3 Influence of exogenous substrates on phosphorylation and dephosphorylation of PAK2

Inside the cell, PAK2 is surrounded with various protein/peptide substrates. Therefore, it is necessary to obtain the information about the effect of exogenous substrates on the autophosphorylation and dephosphorylation of PAK2. Figure 6(a) shows the time courses of enzyme-catalyzed reaction at the different MBP concentrations. From the progress curves of product formation, v_s , α and k_{obs} can be determined by fitting eq. (16) to the experimental data as described before. Figure 6(b) shows the effect of the MBP concentration on the steady-state rate of the enzyme-catalyzed reaction. The steady-state velocity gives rise to the hyperbolic dependence on the MBP concentration. The experimental

data fit the Michaelis-Menten equation with a K_m of $18.0 \pm 1.6 \mu\text{mol/L}$, and k_2 of $4.3 \pm 0.1 \text{ s}^{-1}$. Knowing the value of K_m , the activation rate constants for the free enzyme and enzyme-substrate complex can be obtained from the relationship between k_{obs} and MBP concentration. Figure 6(c) shows a dependence of $A (=k_{\text{obs}}/[T]_0)$ on the substrate concentration. On increasing the concentration of MBP, A decreases and approaches a non-zero constant. The microscopic activation rate constants for the free enzyme, $k_{+0} = 1.39 \pm 0.03 (\mu\text{mol/L})^{-1}\cdot\text{s}^{-1}$, and for the enzyme-substrate complex, $k'_{+0} = 0.24 \pm 0.02 (\mu\text{mol/L})^{-1}\cdot\text{s}^{-1}$, can then be obtained by fitting eq. (18) to the experimental data. As in the case of full-length PAK2, the binding of MBP at the active site of PAK2 does not completely abolish the PAK2 autoactivation even at saturating concentrations of MBP. The microscopic activation rate constant for the free enzyme is about 6-fold greater than that for the enzyme-substrate complex. These data suggest that the binding of MBP only partially inhibit the rate of PAK2 autophosphorylation at site Thr-402.

The time courses of PAK2-catalyzed reaction in the presence of PP1 α as shown in Figure 7(a) are similar to those in the absence of PP1 α . According to the definition of k_{obs}^* , eq. (12) can be rewritten as

$$[P] = \frac{v_s^*}{A[T]_0 - B[M]_0} \ln \left\{ 1 - \frac{\alpha A[T]_0}{A[T]_0 - B[M]_0} \left(1 - e^{(A[T]_0 - B[M]_0)t} \right) \right\}. \quad (19)$$

Similarly, the apparent autophosphorylation rate constant, A , was fixed to a constant value based on the control experiments in the absence of PP1 α , the values of B , α and v_s^* can then be determined by fitting eq. (19) to the experimental data as before. Figure 7(b) shows a plot of the apparent dephosphorylation rate constant, B , against the concentration of MBP. As K_m is known quantity, the microscopic dephosphorylation rate constants for the free enzyme, $k_{-0} = 1.29 \times 10^{-2} \pm 0.03 \times 10^{-2} (\mu\text{mol/L})^{-1}\cdot\text{s}^{-1}$, and for the enzyme-substrate complex, $k'_{-0} = 0.08 \times 10^{-2} \pm 0.002 \times 10^{-2} (\mu\text{mol/L})^{-1}\cdot\text{s}^{-1}$, can then be obtained by fitting eq. (8) to the experimental data.

Small synthetic peptides serve as efficient substrates for a number of protein kinases^[31,32]. To study the effect of different substrates on the PAK2 autoactivation reaction, we used a synthetic peptide derived from myosin II

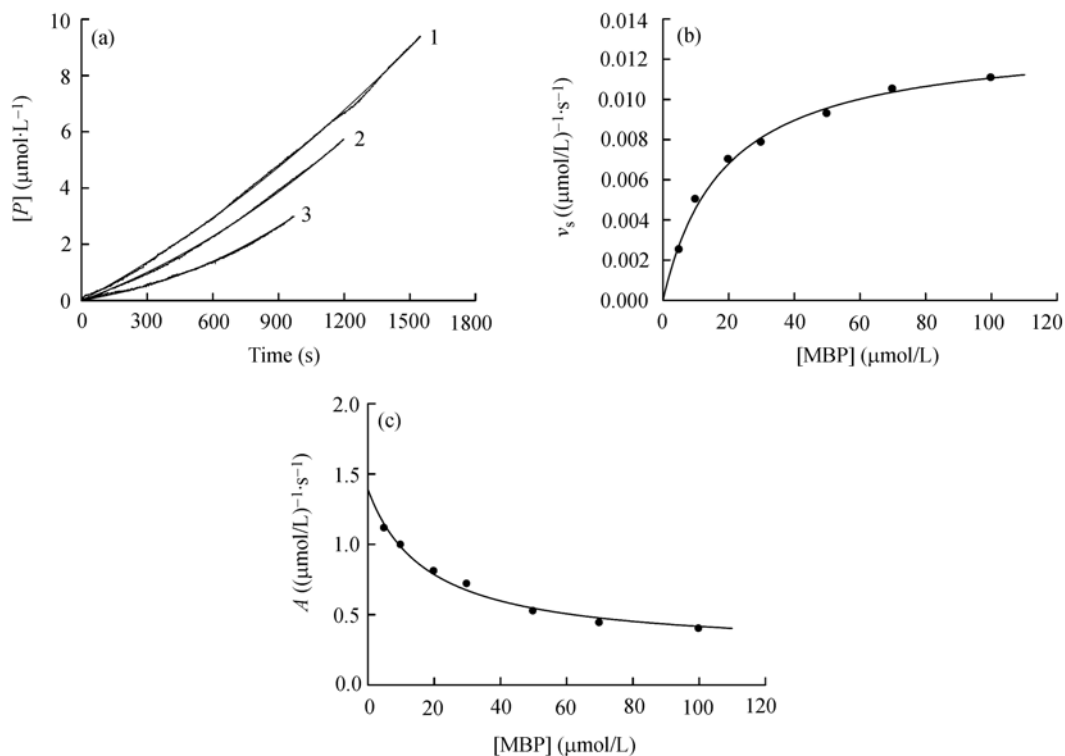


Figure 6 Time course of substrate reaction in the presence of different concentrations of MBP. (a) The reaction was started by the addition of PAK2-p34 to the reaction mixture. The final concentration of PAK2 was 3 nmol/L. Concentrations of MBP were 100, 70, and 30 $\mu\text{mol/L}$ for curves 1–3, respectively. Other conditions were the same as in Figure 3(a). The data were fitted to eq. (16) to determine the kinetic parameters, v_s , A and α . (b) Plot of v_s versus MBP concentration for the autoactivation of PAK2. The solid line represents the best fitting result according to eq. (17) with $K_m=18 \mu\text{mol/L}$, $k_2=4.3 \text{ s}^{-1}$. (c) Plot of A versus MBP concentration for the autoactivation of PAK2. The solid line represents the best fitting result according to eq. (7) with $k_{+0}=1.39 (\mu\text{mol/L})^{-1}\cdot\text{s}^{-1}$, $k'_{+0}=0.24 (\mu\text{mol/L})^{-1}\cdot\text{s}^{-1}$ and $K_m=18 \mu\text{mol/L}$.

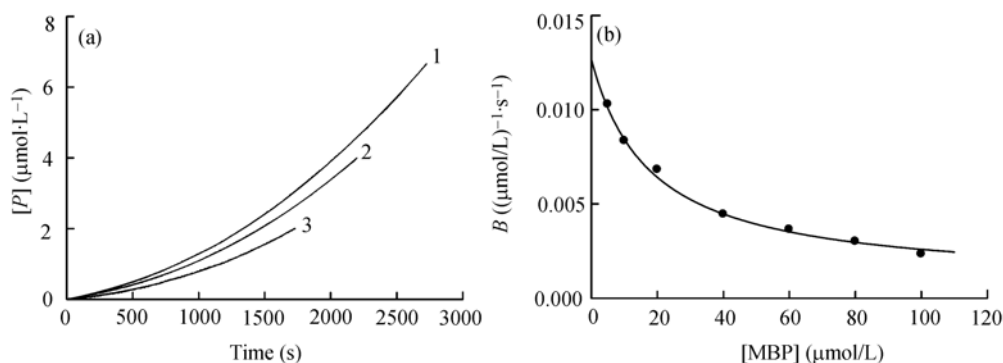


Figure 7 Time course of substrate reaction in the presence of a fixed PP1 α concentration and different MBP concentrations. (a) The reaction was started by the addition of PAK2-p34. The final concentration of PAK2-p34 and PP1 α was 3 nmol/L and 160 nmol/L, respectively. Concentrations of MBP were 80, 60, and 20 $\mu\text{mol/L}$ for curves 1–3, respectively. Other conditions were the same as in Figure 3(a). The data were fitted to eq. (19) to determine the kinetic parameters v_s^* , B and α , where A was calculated according to eq. (7) with $K_m=18 \mu\text{mol/L}$, $k_{+0}=1.39 (\mu\text{mol/L})^{-1}\cdot\text{s}^{-1}$, $k'_{+0}=0.24 (\mu\text{mol/L})^{-1}\cdot\text{s}^{-1}$. (b) Plot of B versus MBP concentration. The solid line represents the best fitting result according to eq. (8) with $k_{-0}=0.0129 (\mu\text{mol/L})^{-1}\cdot\text{s}^{-1}$, $k'_{-0}=0.0008 (\mu\text{mol/L})^{-1}\cdot\text{s}^{-1}$, and $K_m=18 \mu\text{mol/L}$.

Table 1 Kinetic parameters for PAK2 and PP1 α -catalyzed reaction

Kinetic parameter	MBP	RLCtide
k_2 (s^{-1})	4.3 \pm 0.1	13.6 \pm 0.5
K_m ($\mu\text{mol/L}$)	18.0 \pm 1.6	146 \pm 12
k_{+0} ($(\mu\text{mol/L})^{-1}\cdot s^{-1}$)	1.39 \pm 0.03	1.32 \pm 0.02
k_{-0} ($(\mu\text{mol/L})^{-1}\cdot s^{-1}$)	0.24 \pm 0.02	0.31 \pm 0.03
k_{-0} ($(\mu\text{mol/L})^{-1}\cdot s^{-1}$)	(1.29 \pm 0.03) $\times 10^{-2}$	(1.24 \pm 0.02) $\times 10^{-2}$
k'_{-0} ($(\mu\text{mol/L})^{-1}\cdot s^{-1}$)	(7.72 \pm 0.16) $\times 10^{-4}$	(1.09 \pm 0.17) $\times 10^{-3}$
α	0.13 \pm 0.02	0.12 \pm 0.01

regulatory light chain (RLC), RLCtide (residues 11–23, KKRPQRATSNVFA), as a Ser-peptide model substrate. PAK2 can phosphorylate RLC and induce retraction of permeabilized endothelial cells^[33,34]. Similarly, from the progress curves of product formation, all the kinetic parameters for the phosphorylation and dephosphorylation reactions of PAK2 were determined as before, and are summarized in Table 1. It can be seen from this table that although different substrates have vary K_m values, the values of k_{+0} and k_{-0} determined by two different substrates are identical with the experimental error. The consistency of determined rate parameters using MBP and RLCtide as substrates further supports the validity of the new method developed here and the mechanism of Scheme 1 for the PAK2-catalyzed phosphorylation reaction.

4 Discussion

PAK2 undergoes a rapid but transient activation in chemoattractant-stimulated neutrophils with activation/inactivation corresponding to phosphorylation and subsequent dephosphorylation at Thr-402^[35–37]. Thus, phosphatases which catalyze dephosphorylation of the phosphorylated PAK2 are likely to play major roles in regulating this enzyme. Studies with selective inhibitors suggested that a variety of phosphatases might be involved in the rapid dephosphorylation of PAK2 at Thr-402 in stimulated neutrophils^[12]. A variety data implicate PP2A in the dephosphorylation/ inactivation of PAK2. In addition to PP2A, other potential phosphatases that can catalyze this reaction are PP1 and POPX because the sequences surrounding the critical phosphorylation site in the activation loop of PAKs 1–3 are completely homologous. In the present study, PP1 α has been shown to be capable of inactivating the caspase 3-cleaved PAK2 *in vitro* by dephosphorylation of Thr-402 in the activation loop. Analyses of the time courses of PAK2-catalyzed reaction in the absence and presence of

PP1 α suggest that the exogenous substrate has a biphasic effect on the phosphorylation state of PAK2. On the one hand, binding of MBP to the enzyme partially inhibits the rate of its autocatalytic reaction. The second-order rate constants for the activation of caspase 3-cleaved PAK2 determined from these sets of experiments are similar to those of Cdc42-mediated activation of full-length enzyme. On the other hand, binding of MBP to the active site of PAK2 decreases the reaction rate of PP1 α and therefore protects the phospho-residue in the activation loop from the dephosphorylation by PP1 α . The inactivation rate of PAK2-substrate complex by PP1 α is about 10-fold slower than that of the free enzyme, suggesting the phospho-Thr-402 may not be directly involved in PAK2-catalyzed reaction. Therefore, the net effect of MBP on the phosphorylation level of PAK2 will depend on the balance between these two opposing roles.

Recently, Deng et al.^[38] have reported that the full-length and caspase 3-cleaved forms of autophosphorylated MST2, a member of PAK superfamily, display marked difference in susceptibility to protein phosphatases. The full-length phospho-MST2 is rapidly dephosphorylated by protein phosphatase 1 or protein phosphatase 2A whereas the truncated MST2 is remarkably resistant to the dephosphorylation. Therefore, it will be very informative to measure and compare the kinetic parameters for the dephosphorylation reaction of two forms of PAK2 by different phosphatases in a future study. Continued study on the role of PP1 α , PP2A and POPX and how they act together with PAKs to regulate the PAK pathway should provide further insights into the regulation of PAK pathways by protein phosphatases.

We would like to thank Xiu-Jie Xie (Beijing Normal University) for assistance of PP1 α purification.

- 1 Bokoch G M. Biology of the p21-activated kinases. *Annu Rev Biochem*, 2003, 72: 743—781
- 2 Lim L, Manser E, Leung T, et al. Regulation of phosphorylation pathways by p21 GTPases. The p21 Ras-related Rho subfamily and its role in phosphorylation signalling pathways. *Eur J Biochem*, 1996, 242: 171—185
- 3 Sells M A, Chernoff J. Emerging from the Pak: the p21-activated protein kinase family. *Trends Cell Biol*, 1997, 7: 162—167
- 4 Bagrodia S, Cerione R A. Pak to the future. *Trends Cell Biol*, 1999, 9: 350—355
- 5 Rudel T, Bokoch G M. Membrane and morphological changes in apoptotic cells regulated by caspase-mediated activation of PAK2. *Science*, 1997, 276: 1571—1574
- 6 Walter B N, Huang Z, Jakobi R, et al. Cleavage and activation of p21-activated protein kinase gamma-PAK by CPP32 (caspase 3). Effects of autophosphorylation on activity. *J Biol Chem*, 1998, 273: 28733—28739
- 7 Jakobi R, McCarthy C C, Koeppl M A, et al. Caspase-activated PAK-2 is regulated by subcellular targeting and proteasomal degradation. *J Biol Chem*, 2003, 278: 38675—38685
- 8 Koeppl M A, McCarthy C C, Moertl E, et al. Identification and characterization of PS-GAP as a novel regulator of caspase-activated PAK-2. *J Biol Chem*, 2004, 279: 38653—38664
- 9 Barford D. Molecular mechanisms of the protein serine/threonine phosphatases. *Trends Biochem Sci*, 1996, 21: 407—412
- 10 Ceulemans H, Bollen M. Functional diversity of protein phosphatase-1, a cellular economizer and reset button. *Physiol Rev*, 2004, 84: 1—39
- 11 Westphal R S, Coffee R L, Marotta Jr A, et al. Identification of kinase-phosphatase signaling modules composed of p70 S6 kinase-protein phosphatase 2A(PP2A) and p21-activated kinase-PP2A. *J Biol Chem*, 1999, 274: 687—692
- 12 Zhan Q, Ge Q, Ohira T, et al. p21-activated kinase 2 in neutrophils can be regulated by phosphorylation at multiple sites and by a variety of protein phosphatases. *J Immunol*, 2003, 171: 3785—3793
- 13 Koh C G, Tan E J, Manser E, et al. The p21-activated kinase PAK is negatively regulated by POPX1 and POPX2, a pair of serine/threonine phosphatases of the PP2C family. *Curr Biol*, 2002, 12: 317—321
- 14 Tsou C L. Kinetics of substrate reaction during irreversible modification of enzyme activity. *Adv Enzymol*, 1988, 61: 381—436
- 15 Wang Z X, Zhou B, Wang Q M, et al. A kinetic approach for the study of protein phosphatase-catalyzed regulation of protein kinase activity. *Biochemistry*, 2002, 41: 7849—7857
- 16 Wu H, Wang Z X. The mechanism of p21-activated kinase 2 autoactivation. *J Biol Chem*, 2003, 278: 41768—41778
- 17 Killilea S D, Cheng Q, Wang Z X. Protein phosphatase type 1 and type 2A assays. *Methods Mol Biol*, 1998, 93: 23—33
- 18 Wu H, Zheng Y, Wang Z X. Evaluation of the catalytic mechanism of the p21-activated protein kinase PAK2. *Biochemistry*, 2003, 42: 1129—1139
- 19 Zhang Z, Bai G, Deans-Zirattul S, et al. Expression of the catalytic subunit of phosphorylase phosphatase (protein phosphatase-1) in *Escherichia coli*. *J Biol Chem*, 1992, 267: 1484—1490
- 20 Mittl P R E, Di Marco S, Krebs J F, et al. Structure of recombinant human CPP32 in complex with the tetrapeptide acetyl-Asp-Val-Ala-Asp fluoromethyl ketone. *J Biol Chem*, 1997, 272: 6539—6547
- 21 Prowse C N, Hagopian J C, Cobb M H, et al. Catalytic reaction pathway for the mitogen-activated protein kinase ERK2. *Biochemistry*, 2000, 39: 6258—6266
- 22 Gill S C, Hippel P H. Calculation of protein extinction coefficients from amino acid sequence data. *Anal Biochem*, 1989, 182: 319—326
- 23 Zhou B, Zhang Z Y. Mechanism of mitogen-activated protein kinase phosphatase-3 activation by ERK2. *J Biol Chem*, 1999, 274: 35526—35534
- 24 Cheng Q, Wang Z X, Killilea S D. A continuous spectrophotometric assay for protein phosphatases. *Anal Biochem*, 1995, 226: 68—73
- 25 Zhou B, Wang Z X, Zhao Y, et al. The specificity of extracellular signal-regulated kinase 2 dephosphorylation by protein phosphatases. *J Biol Chem*, 2002, 277: 31818—31825
- 26 Webb M R. A continuous spectrophotometric assay for inorganic phosphate and for measuring phosphate release kinetics in biological systems. *Proc Natl Acad Sci USA*, 1992, 89: 4884—4887
- 27 Cook P F, Neville M E Jr, Vrana K E, et al. Adenosine cyclic 3', 5'-monophosphate dependent protein kinase: Kinetic mechanism for the bovine skeletal muscle catalytic subunit. *Biochemistry*, 1982, 21: 5794—5799
- 28 Tuazon P T, Spanos W C, Gump E L, et al. Determinants for substrate phosphorylation by p21-activated protein kinase (γ PAK). *Biochemistry*, 1997, 36: 16059—16064
- 29 Gatti A, Huang Z, Tuazon P T, et al. Multisite autophosphorylation of p21-activated protein kinase γ -PAK as a function of activation. *J Biol Chem*, 1999, 274: 8022—8028
- 30 Zhao Z S, Manser E, Chen X Q, et al. A conserved negative regulatory region in α PAK: Inhibition of PAK kinases reveals their morphological roles downstream of Cdc42 and Rac1. *Mol Cell Biol*, 1998, 18: 2153—2163
- 31 Kemp B E, Pearson R B. Protein kinase recognition sequence motifs. *Trends Biochem Sci*, 1990, 15: 342—346
- 32 Kemp B E, Parker M W, Hu S, et al. Substrate and pseudosubstrate interactions with protein kinases: Determinants of specificity. *Trends Biochem Sci*, 1994, 19: 440—444
- 33 Chew T L, Masaracchia R A, Goeckeler Z M, et al. Phosphorylation of non-muscle myosin II regulatory light chain by p21-activated kinase (γ -PAK). *J Muscle Res Cell Motil*, 1998, 19: 839—854
- 34 Zeng Q, Lagunoff D, Masaracchia R, et al. Endothelial cell retraction is induced by PAK2 monophosphorylation of myosin II. *J Cell Sci*, 2000, 113: 471—482
- 35 Lian J P, Toker A, Badwey J A. Phosphorylation of the activation loop of gamma p21-activated kinase (γ -Pak) and related kinases (MSTs) in normal and stressed neutrophils. *J Immunol*, 2001, 166: 6349—6357
- 36 Ding J, Badwey J A. Stimulation of neutrophils with a chemoattractant activates several novel protein kinases that can catalyze the phosphorylation of peptides derived from the 47-kDa protein component of the phagocyte oxidase and myristoylated alanine-rich C kinase substrate. *J Biol Chem*, 1993, 268: 17326—17333
- 37 Huang R, Lian J P, Robinson D, et al. Neutrophils stimulated with a variety of chemoattractants exhibit rapid activation of p21-activated kinases (Paks): Separate signals are required for activation and inactivation of paks. *Mol Cell Biol*, 1998, 18: 7130—7138
- 38 Deng Y, Pang A, Wang J H. Regulation of mammalian STE20-like kinase 2 (MST2) by protein phosphorylation/dephosphorylation and proteolysis. *J Biol Chem*, 2003, 278: 11760—11767